applied sciences

MDPI

Article

Overload Control in Smart Transformer-Fed Grid

Giovanni De Carne [1,*], Zhixiang Zou [1], Giampaolo Buticchi [1], Marco Liserre [1] and Costas Vournas [2]

[1] Power Electronics, Christian-Albrechts University of Kiel, Kiel D-24143, Germany; zz@tf.uni-kiel.de (Z.Z.); gibu@tf.uni-kiel.de (G.B.); ml@tf.uni-kiel.de (M.L.)

[2] School of Electrical and Computer Engineering, National Technical University of Athens, Athens 157 80, Greece; vournas@power.ece.ntua.gr

* Correspondence: gdc@tf.uni-kiel.de; Tel.: +49-431-8806-107

Academic Editors: Frede Blaabjerg and Yongheng Yang

Received: 9 December 2016; Accepted: 13 February 2017; Published: 20 February 2017

Abstract: Renewable energy resources and new loads—such as electric vehicles—challenge grid management. Among several scenarios, the smart transformer represents a solution for simultaneously managing low- and medium-voltage grids, providing ancillary services to the distribution grid. However, unlike conventional transformers, the smart transformer has a very limited overload capability, because the junction temperature—which must always be below its maximum limit—is characterized by a short time constant. In this work, an overload control for smart transformer by means of voltage and frequency variations has been proposed and verified by means of simulations and experiments.

Keywords: smart transformer; solid state transformer; overload control; voltage control; frequency control

1. Introduction

The integration of new loads (e.g., electric vehicles) challenges distribution grid management in several aspects, such as phases imbalance, power quality issues, and transformer overload. The last aspect is important concerning the installation of electric vehicle (EV) charging stations [1]. Even in the case of the limited integration of EVs, the transformer overloads more frequently than the purely passive load case [2]. Of particular concern is uncontrolled EV charging. In a possible initial implementation scenario, the overload conditions can occur in up to 40% of the cases. Under controlled charging, the overload cases can be reduced to 20%. The conventional transformers are designed for handling higher power than the nominal one. Their overload capability depends on the highest temperature (hot spot), and short term overload is permitted for a few hours per day [3,4].

The smart transformer (ST) is a power electronics-based transformer [5] that aims not only at adapting the voltage level from medium voltage (MV) to low voltage (LV), but at providing new services to the distribution grids: load identification and control [6,7], reverse power flow controller [8], reactive power support in MV grid [9], power management in the DC grid [10], and grid hosting capacity increase for photovoltaics (PV) and the integration of electric vehicle charging stations [11]. The ST—in contrast to the conventional transformer—has a limited overload capability. Its overload capability has been accounted for the 120% of nominal current rating for a short time window in [12]. However, a current higher than the nominal one may impact on the ST lifetime.

In this paper, a ST overload control is proposed based on the interaction with the local loads and generators in an LV grid by means of voltage and frequency signals. The idea was already proposed in [13,14]; however, in this paper, it is described in more detail and verified by means of PSCAD/EMTDC^{TM} simulations and lab experiments. When approaching the overload condition,

the ST decreases the frequency in order to increase the local generators power output, if equipped with droop controllers. In the case of insufficient power handling capability of these resources, the ST resorts to the voltage controller. Decreasing the voltage, the load reduces the power absorption, avoiding the overload condition. The sensitivity of load active power to voltage is assumed unknown a priori throughout this study. It should be noted, however, that this can be measured on-line using the method introduced in [6,7]—in which case the active load control through voltage setpoint manipulation becomes more accurate. In this paper, the assumption of constant impedance load is made in order to simplify the experimental validation of the method by means of a lab setup. This assumption does not affect the generality of the approach, once the load coefficient sensitivity are computed following [6].

Similar methods have been applied for energy saving purposes, such as the Conservation Voltage Reduction (CVR) method [15,16]. Unlike the proposed overload controller, the CVR is applied in steady state and not during transients, and the current value is not controlled during the voltage variation. A possible solution to solve the conventional transformer overload is given in [17]: the transformer tap changer and the implementation of P/V droop controller in the Distributed Generation (DG) has been used to modify the voltage and following the power injection of DG in a microgrid. The current literature on ST is more focused on fault handling more than in the overload transients. To the authors' knowledge, no extensive research has been performed until now regarding the overload control of the ST or solid state transformer (SST) LV side. Particular emphasis has been given in the existing literature to the ST MV converter protection, more than in the overload condition. In [18], protection schemes against overvoltage and short circuits in MV grid are extensively discussed, and in [19] an SST-based protection scheme against short circuits has been proposed for LV grids.

This paper is structured as follows: Section 2 gives an overview of the ST concept and control, including the proposed overload controller; Section 3 describes the grid simulated in PSCAD; the simulation results of the grid are shown in Section 4; and the experimental verification is performed in Section 5. Section 6 is dedicated to the conclusions.

2. Smart Transformer Concept and Control

The smart transformer proposed in this work is a three-stage power electronics transformer [5,20]. The ST adapts the voltage between the MV to the LV grid, and enables the DC grid connections at both voltage levels [21]. A reference system is shown in Figure 1. Several topology solutions can be implemented for each stage, although the control strategies do not differ substantially. The ST control strategy adopted in this work is shown in Figure 2.

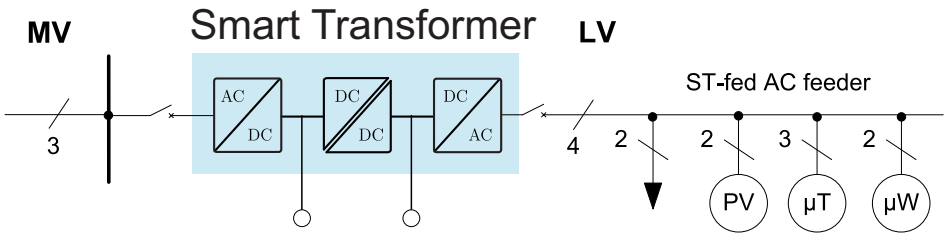

Figure 1. Smart transformer (ST) concept. LV: low voltage; MV: medium voltage; PV: photovoltaic; μT: micro-turbine; μW: micro-wind turbine.

The MV side regulates the MV DC link voltage at the nominal value, controlling the active current absorption in the MV grid. The reactive power injection in the MV grid is controlled in order to provide reactive power support in MV grid. The ST has the possibility of working under constant power factor, or to support the voltage profile by injecting reactive power. The reactive power control can be local by means of a V/Q droop controller, or remote using a centralized controller.

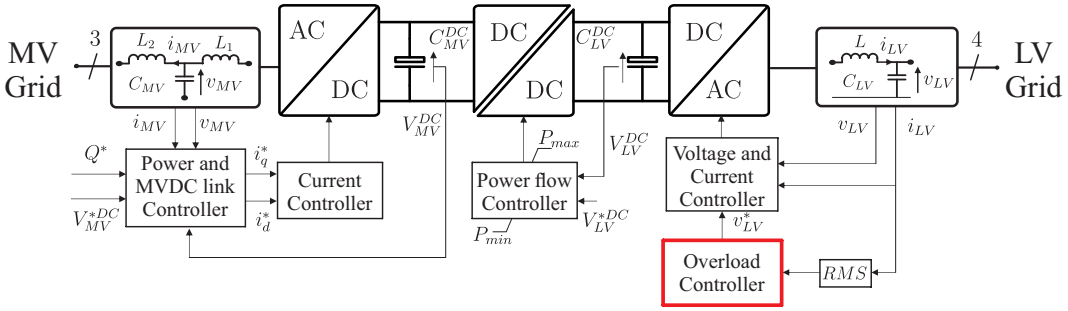

Figure 2. Smart transformer control scheme and proposed controller to avoid overload condition (red square). RMS: root mean square.

The DC/DC converter has the task of transforming the voltage from MV to LV and to control the LV DC link voltage. The DC/DC controls the power flow between the two voltage levels in order to keep the LV DC link voltage at its nominal value. The reference power is limited between the P_{max} (determined by the ST sizing) and P_{min}. In order to prevent reverse power flow, P_{min} must be set to zero.

The LV side controls the LV grid voltage waveform. It provides symmetrical voltage waveforms with constant amplitude and frequency, independently from the load power request. The current amplitude and shape is instead decided solely by the load. In this work, the voltage waveform reference is given by the overload controller (Figure 2, red box), explained in the next section.

Smart Transformer Overload Controller

In this paper, the ST overload controller is implemented in the LV side voltage controller. The ST measures the current root mean square (RMS) value and sets two current thresholds for the frequency and voltage controller, respectively. As shown in Figure 3, the frequency controller is activated as soon as the rms current exceeds the 80% of the maximum current limit, set as the current at ST nominal power and voltage. If the controllable resources size is not sufficient or the controller hits the minimum frequency limit (e.g., 49 Hz), the current rises until it reaches 90% of the maximum limit and activates the voltage controller. Here, the ST decreases the voltage amplitude to keep the current within the allowable range. In case the current reaches the maximum current limit—despite the overload controller action—the system resorts to load shedding in the LV grid. In the case of emergency, the ST is forced to shut down in order to avoid hardware damage. As soon as the ST current decreases, the voltage controller at first, followed by the frequency controller, deactivate. In the voltage controller, a rate limiter has been implemented in order to avoid disruptive interactions with the frequency controller during the voltage recovery. If the voltage controller is too fast in recovering the grid voltage, the frequency controller may oscillate, destabilizing the system.

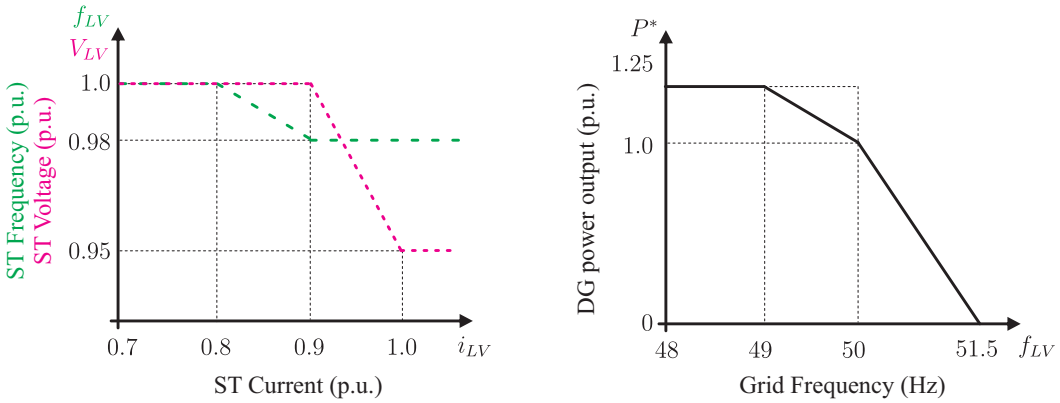

Figure 3. ST overload controller and DG (Distributed Generation) droop controller.

In the controllable resources, a droop controller curve is implemented as shown in Figure 3. The interface converter decreases its power output until shut down in the case of high frequency (51.5 Hz) [22] and increases its power injection up to 125% in the case of frequency decrease (49 Hz). Implementing such droop controller, the interface converter can interact with the ST under frequency variation signals. The frequency threshold values chosen for this work respects what asked in the Italian standard [22]. The DG converter must remain connected to the grid within the frequency range (47.5–51.5) Hz. In case of over-frequency, the DG must reduce the power output from nominal power (50.3 Hz) to zero power (51.5 Hz). It is worth mentioning that this controller does not affect MV and high voltage (HV) grids. The ST is a three-stage power electronics-based transformer with two DC links. This enables an AC power flow separation between the LV and MV grids; thus, the frequency change in the LV grid is independent from the MV grid frequency.

The frequency controller may, however, impact digital clocks based on the grid frequency, causing a time drift due to the variable frequency. The ST can provide an isochronous control based on universal time signal in order to reset the frequency-based clocks on a daily basis. In this way, the error introduced by variable frequency control can be corrected.

3. Grid under Test

The simulations are carried out implementing a modified CIGRE European LV distribution network benchmark [23] (Figure 4) in PSCAD/EMTDC^{TM} v46. The assumptions made in this work are as follows: (1) the loads are balanced three-phase; (2) the distributed resources, such as Battery Energy Storage Systems (BESS) and PV are working with unity power factor; (3) the wind turbine has been removed; (4) the loads are assumed as constant impedance by means of an exponential load model. The load and ST data are listed in Table 1. The battery energy systems and the photovoltaic power plants are controlled by means of an external power loop that gives the reference current to a current loop. The nominal data of the batteries and PV are listed in in Table 2. The energy resource models are tuned following the standard procedures for renewable converters described in [24].

Table 1. Load and ST (smart transformer) data.

Load	Bus	Nominal Power (kW)	cos φ	ST Parameter	Value
L1	11	20.0	0.90	ST_{size}	120 kVA
L2	15	10.0	0.90	V_{LV}^{DC}	800 V
L3	16	10.0	0.90	C_{LV}^{DC}	2.0 mF
L4	17	25.0	0.90	L_{LV}	8.0 mH
L5	18	15.0	0.90	C_{LV}	50.0 µF

Table 2. BESS (Battery Energy Storage Systems) and PV (photovoltaics) data.

Resource	Nominal Power (kVA)
BESS A	35
BESS B	25
PV A	4
PV B	3

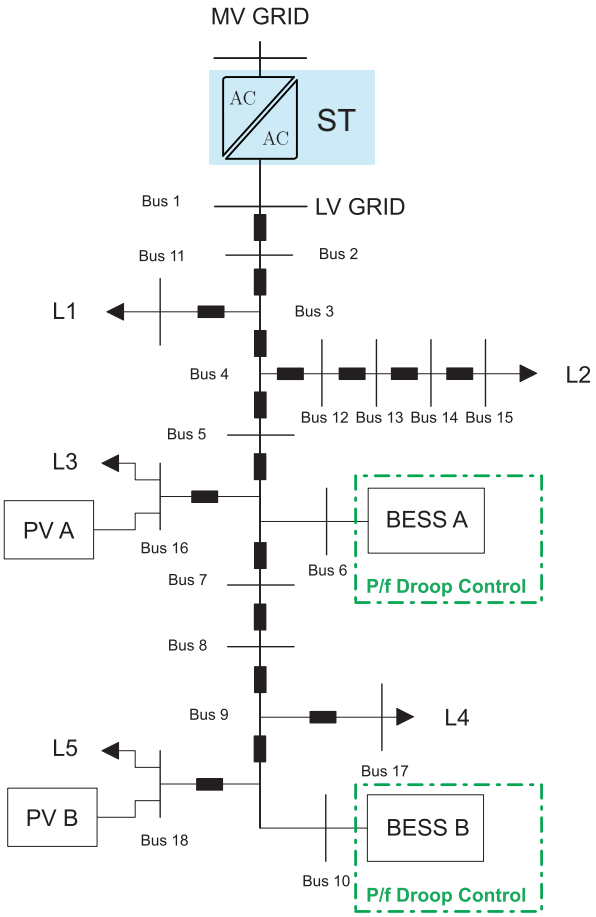

Figure 4. Grid simulated in PSCAD/EMTDC™.

4. Simulation Results

The simulations were carried out implementing the grid described in the previous section in PSCAD. The maximum current allowable in the ST is 174 A, corresponding to the current flowing in the ST working at nominal power (120 kVA) under nominal voltage (230 V_{rms}). The sum of the load and BESS profiles are shown in Figure 5. Without losing generality on the methodology, a unique load profile for the loads has been considered. The voltage controller ramp limiter has been set in this simulation to 0.5 V/s.

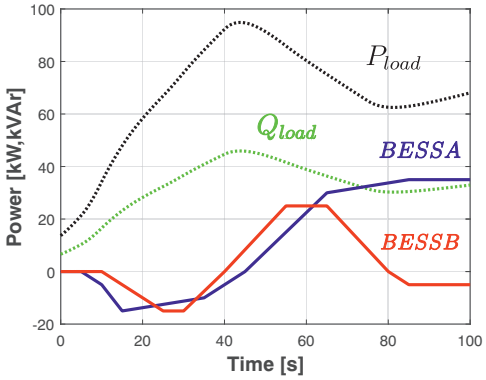

Figure 5. BESS *A* active power (blue line), BESS *B* active power (red line), sum of load active power (dotted black line), sum of load reactive power (dotted green line).

The frequency controller is activated when the current goes above the 80% threshold and the voltage controller follows at 90% of the nominal current. In Figure 6a, the current profile in absence of overload control is plotted (black line). As can be noted, without control, the current exceeds the current maximum limit for more than 20 s in the considered time window. This may lead to damages to power semiconductor and reduction of the ST expected lifetime.

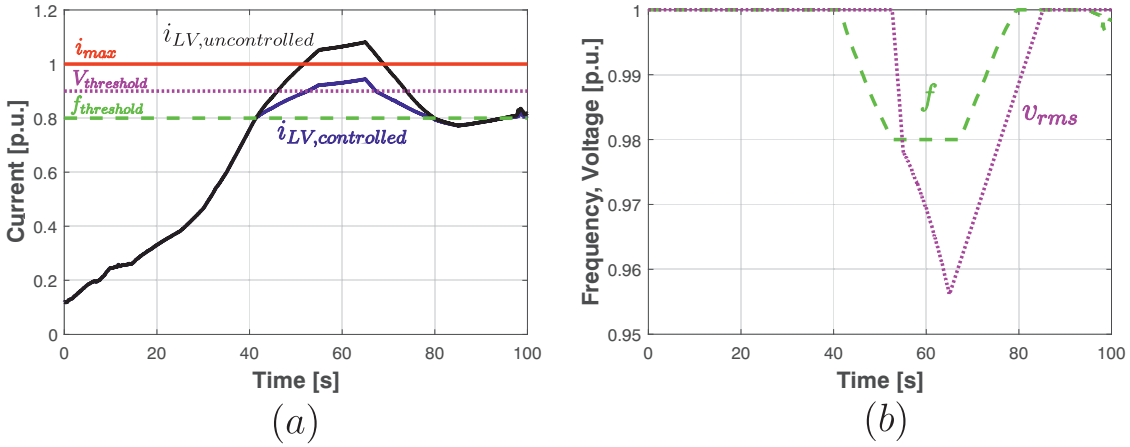

Figure 6. Overload controller simulations: (**a**) ST current without controller (black line), ST current with the proposed overload controller (blue line), frequency controller threshold (dashed green line), voltage controller threshold (dotted magenta line), current maximum limit (red line); (**b**) grid frequency (dashed green line), ST bus voltage (dotted magenta line).

Applying the ST overload controller, the current is kept below the maximum limit. As plotted in Figure 6, as soon as the current exceeds the frequency threshold, the ST decreases the output frequency until reaching the minimum value of 0.98 p.u. (49 Hz). The current slope is decreased with respect to the no-control case, but due to the limited amount of controllable resources, the current still exceeds the voltage threshold. Here, the voltage amplitude is decreased in order to reduce the load's power consumption. It can be noted in Figure 6 how the current is controlled below the current maximum limit and the voltage is decreased till 0.955 p.u., while the frequency is kept constant to 49 Hz. When the overload condition is solved and the load power request is decreased, the ST restores the voltage to the nominal voltage and controls the current profile with the frequency controller. Until the overload is not completely solved, the ST maintains the frequency controller in the activated state.

The batteries' power profiles are shown in Figure 7a. The batteries increase the power output when the frequency is modified due to the droop controller action (solid lines) with respect to the base

case (dotted lines). The effectiveness of the combined action of frequency and voltage controllers can be observed in the ST power profiles in Figure 7b. Without control, the active power alone exceeds the ST size (dotted black line). Applying the ST overload control, both active and reactive power are reduced (continuous lines).

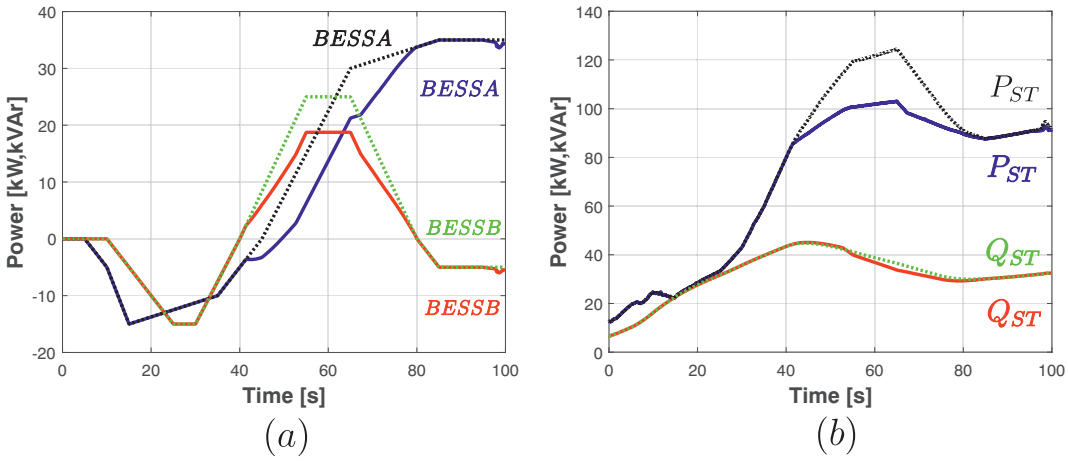

Figure 7. (**a**) Active power without controller BESS *A* (dotted green line), with overload controller (red line), active power without controller BESS *B* (dotted black line), with overload controller (blue line); (**b**) ST: Active power without controller (dotted black line), with overload controller (blue line), reactive power without controller (dotted green line), with overload controller (red line).

5. Experimental Results

The overload controller simulated in the previous section has been experimentally verified with the microgrid setup shown in Figure 8. The experimental setup is composed of two three-phase voltage source converters (VSCs) (Danfoss Converter 4 kW) and a variable resistor used to create the overload conditions. The controller of the inverter emulating the ST has been implemented as described in Figure 2. The experimental setup parameters are listed in Table 3, and the controllers of both inverters are implemented in a dSPACE 1106.

In the DG side converter, the droop controller described in Figure 3 has been implemented.

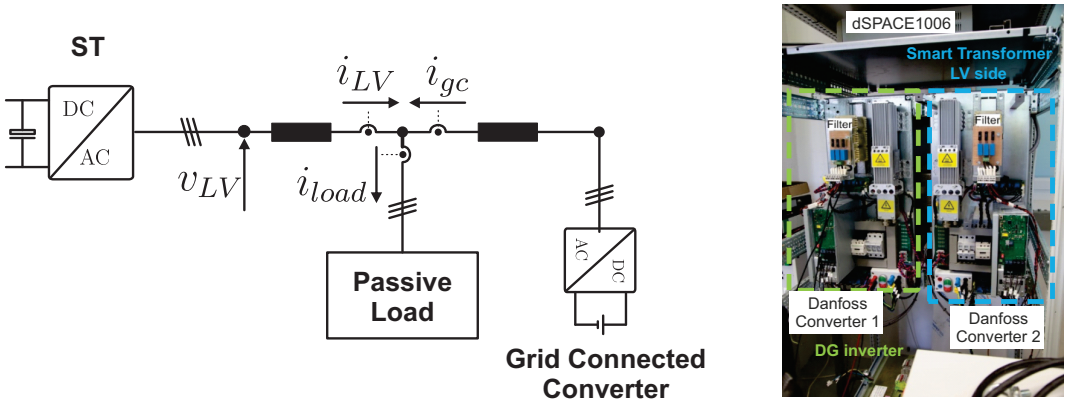

Figure 8. Lab experimental setup scheme and picture.

Table 3. Experimental setup parameters.

Parameter	Value	Parameter	Value
V_{LV}^{DC}	650 V	V_{DG}^{DC}	650 V
C_{LV}^{DC}	3.3 mF	L_f	5.03 mH
C_f	10 µF	v_{LV}	220 V_{rms}
f_s	10 kHz	i_{max}	6 A

The maximum current has been set to 6 A_{rms}, and the frequency and voltage controller threshold have been set to 80% and 90%, respectively. The voltage controller ramp limiter has been set equal to 0.2 V/s. The variable resistor has been operated from 28 Ω to 21 Ω for about 20 s. In Figure 9 the operations of the overload controller have been plotted. As soon as the ST current exceeds the 4.8 A threshold, the frequency controller is activated, and it decreases the frequency from 50 Hz to 49 Hz. When the current increases above 5.4 A the voltage is decreased, limiting the ST overload to 5.6 A, with a further margin for load increase. The voltage drops from 220 V to 215.5 V during the steady state condition. As soon as the variable resistance increases, the ST current decreases, and the voltage and frequency are slowly restored to the nominal value. A better understanding of the overload controller operations can be obtained looking at Figures 10 and 11. These figures represent the steady-state waveforms before the overload condition and during the controller operation, marked respectively with the orange and green boxes in Figure 9. In Figure 10, the ST controls the voltage waveform v_{LV} at the nominal amplitude and frequency, being the ST current i_{LV} lower than the frequency controller threshold. The DG current i_{gc} amounts to 4 A_{peak} and the load absorbing about $i_{load} = 11\ A_{peak}$. As soon as the load increases, the overload controller acts on the voltage amplitude and frequency values. The steady-state behavior during the controller operations (Figure 9, green box) is shown in Figure 11. The ST decreases the voltage v_{LV} amplitude and frequency, and the DG is able to recognize the frequency change and increase the current output up to 5 A_{peak}. The load current consumption is maintained at 14.4 A_{peak} by the voltage controller, instead to increase to 14.8 A_{peak}. Both frequency and voltage controllers are able to avoid the ST overload.

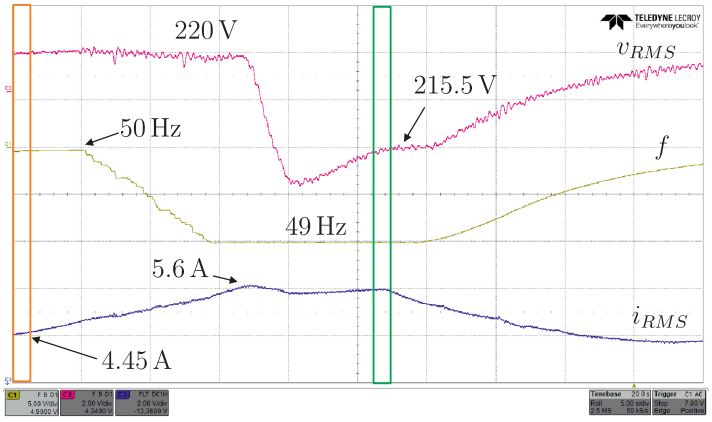

Figure 9. Experimental results: ST rms voltage v_{LV} (magenta line), grid frequency f_{LV}(yellow line), and ST rms current i_{LV} (blue line).

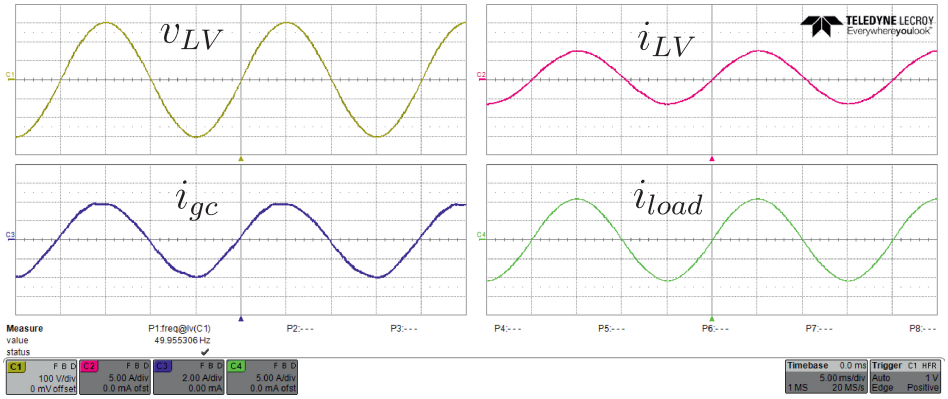

Figure 10. Steady-state before the overload (Figure 9, orange box): ST voltage (yellow line, 100 V/div), ST current (magenta line, 5 A/div), DG current (blue line, 2 A/div), load current (green line, 5 A/div).

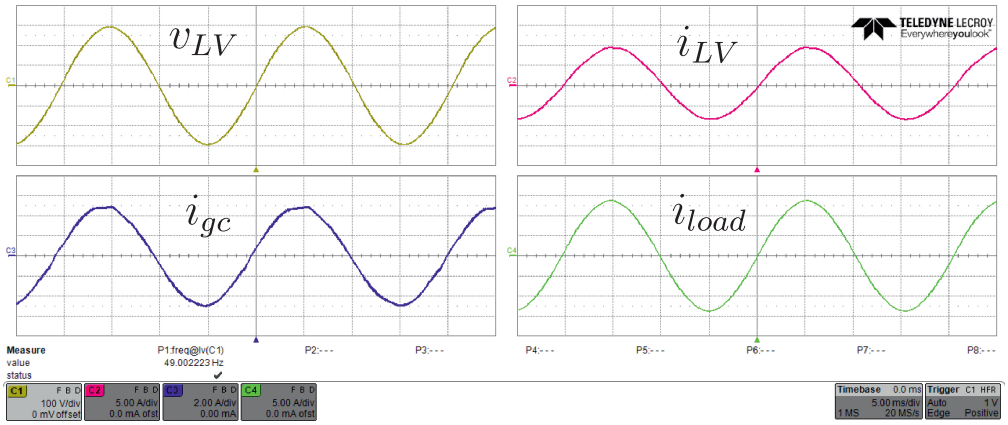

Figure 11. Steady-state during the overload controller operations (Figure 9, green box): ST voltage (yellow line, 100 V/div), ST current (magenta line, 5 A/div), DG current (blue line, 2 A/div), load current (green line, 5 A/div).

6. Conclusions

The smart transformer is a power electronics-based transformer. Its overload capability is limited by the semiconductor temperature, and it allows only small overload for very short time (few µs). This paper proposes an overload control for smart transformer applications. The main idea is to interact with the local loads and generators in an LV grid by means of voltage and frequency variations in order to limit the current flowing in the ST. The DG—if controllable and equipped with droop controller—is able to increase the power injection, measuring the controlled frequency decrease in the LV grid. In case of insufficient control capability of the frequency controller, the voltage controller is activated. It acts directly on the loads, exploiting the load power sensitivity to voltage variations. Decreasing the voltage, the voltage controller decreases the power consumption in the grid, limiting the ST overload. The simulation and experimental results show how the proposed controller manages the overload conditions by interacting with local loads and controllable resources.

A future research direction will directly consider the devices' temperature instead of the current. In this way, the on-line ST current capacity can be estimated more accurately. Further studies investigating the robustness of the solution against the load composition must be carried out to make the solution ready for a real grid scenario. The overload controller can be affected if the load compositions varies too rapidly, imposing the wrong voltage variation direction (e.g., from decreasing the voltage for constant impedance to increasing it for constant power loads).

Acknowledgments: The research leading to these results has received funding from the European Research Council under the European Union's Seventh Framework Programme (FP/2007–2013) / ERC Grant Agreement n. [616344]—HEART.

Author Contributions: Giovanni De Carne, Zhixiang Zou and Giampaolo Buticchi conceived, designed and performed the experiments; Marco Liserre and Costas Vournas analyzed the data; Giovanni De Carne wrote the paper.

Conflicts of Interest: The authors declare no conflict of interest.

References

1. Liu, R.; Dow, L.; Liu, E. A survey of PEV impacts on electric utilities. In Proceedings of the 2011 IEEE PES Innovative Smart Grid Technologies (ISGT), Hilton Anaheim, CA, USA, 17–19 January 2011; pp. 1–8.
2. Verzijlbergh, R.A.; Grond, M.O.W.; Lukszo, Z.; Slootweg, J.G.; Ilic, M.D. Network Impacts and Cost Savings of Controlled EV Charging. *IEEE Trans. Smart Grid* **2012**, *3*, 1203–1212.
3. Fu, W.; McCalley, J.D.; Vittal, V. Risk assessment for transformer loading. *IEEE Trans. Power Syst.* **2001**, *16*, 346–353.
4. Weekes, T.; Molinski, T.; Swift, G. Transient transformer overload ratings and protection. *IEEE Electr. Insul. Mag.* **2004**, *20*, 32–35.
5. Liserre, M.; Buticchi, G.; Andresen, M.; Carne, G.D.; Costa, L.F.; Zou, Z.X. The Smart Transformer: Impact on the Electric Grid and Technology Challenges. *IEEE Ind. Electron. Mag.* **2016**, *10*, 46–58.
6. De Carne, G.; Liserre, M.; Vournas, C. On-line load sensitivity identification in LV distribution grids. *IEEE Trans. Power Syst.* **2016**, doi:10.1109/TPWRS.2016.2581979.
7. De Carne, G.; Buticchi, G.; Liserre, M.; Vournas, C. Load Control using Sensitivity Identification by means of Smart Transformer. *IEEE Trans. Smart Grid* **2016**, doi:10.1109/TSG.2016.2614846.
8. Buticchi, G.; Carne, G.D.; Barater, D.; Zou, Z.; Liserre, M. Analysis of the Frequency-Based Control of a Master/Slave Micro-Grid. *IET Renew. Power Gener.* **2016**, *10*, 1570–1576.
9. Huang, A.Q. Medium-Voltage Solid-State Transformer: Technology for a Smarter and Resilient Grid. *IEEE Ind. Electron. Mag.* **2016**, *10*, 29–42.
10. Yu, X.; She, X.; Zhou, X.; Huang, A. Power Management for DC Microgrid Enabled by Solid-State Transformer. *IEEE Trans. Smart Grid* **2014**, *5*, 954–965.
11. Huang, S.; Pillai, J.; Liserre, M.; Bak-Jensen, B. Improving photovoltaic and electric vehicle penetration in distribution grids with smart transformer. In Proceedings of the 4th Innovative Smart Grid Technologies Europe (ISGT EUROPE), Lyngby, Denmark, 6–9 October 2013; pp. 1–5.
12. Carr, J.; Wang, Z.; Bhattacharya, S.; Hatua, K.; Madhusoodhanan, S. Overloading and overvoltage evaluation of a Transformerless Intelligent Power Substation. In Proceedings of the 2013 IEEE Power Energy Society General Meeting, Vancouver, BC, Canada, 21–25 July 2013; pp. 1–5.
13. De Carne, G.; Buticchi, G.; Liserre, M.; Marinakis, P.; Vournas, C. Coordinated Frequency and Voltage Overload Control of Smart Transformers.In Proceedings of the IEEE PowerTech, Eindhoven, The Netherlands, 29 June–2 July 2015.
14. De Carne, G.; Buticchi, G.; Liserre, M.; Vournas, C. Frequency-Based Overload Control of Smart Transformers. In Proceedings of the IEEE PowerTech, Eindhoven, The Netherlands, 29 June–2 July 2015.
15. Schneider, K.P.; Fuller, J.; Tuffner, F.; Singh, R. *Evaluation of Conservation Voltage Reduction (CVR) on a National Level*; Technical Report; Pacific Northwest National Laboratory: Oak Ridge, TN, USA, 2010.
16. Wang, Z.; Wang, J. Review on Implementation and Assessment of Conservation Voltage Reduction. *IEEE Trans. Power Syst.* **2014**, *29*, 1306–1315.
17. Vandoorn, T.L.; Kooning, J.D.; Meersman, B.; Guerrero, J.M.; Vandevelde, L. Voltage-Based Control of a Smart Transformer in a Microgrid. *IEEE Trans. Ind. Electron.* **2013**, *60*, 1291–1305.
18. Guillod, T.; Krismer, F.; Kolar, J. Protection of MV Converters in the Grid: The Case of MV/LV Solid-State Transformers. *IEEE J. Emerg. Sel. Top. Power Electron.* **2016**, *5*, 393–408.
19. Tatcho, P.; Li, H.; Jiang, Y.; Qi, L. A Novel Hierarchical Section Protection Based on the Solid State Transformer for the Future Renewable Electric Energy Delivery and Management (FREEDM) System. *IEEE Trans. Smart Grid* **2013**, *4*, 1096–1104.

20. She, X.; Huang, A.; Burgos, R. Review of Solid-State Transformer Technologies and Their Application in Power Distribution Systems. *IEEE J. Emerg. Sel. Top. Power Electron.* **2013**, *1*, 186–198.
21. She, X.; Huang, A.Q.; Lukic, S.; Baran, M.E. On Integration of Solid-State Transformer with Zonal DC Microgrid. *IEEE Trans. Smart Grid* **2012**, *3*, 975–985.
22. Comitato Elettrotecnico Italiano (CEI). *Reference Technical Rules for the Connection of Active and Passive Users to the LV Electrical Utilities*; CEI: Milano, Italy, 2012.
23. CIGRE. *Benchmark System for Network Integration of Renewable and Distributed Energy Resources C06.04.02*; Technical Report; CIGRE: Paris, France, 2014.
24. Teodorescu, R.; Liserre, M.; Rodriguez, P. *Grid Converters for Photovoltaic and Wind Power Systems*; Wiley: Hoboken, NJ, USA, 2011.